Proceedings of the 11th ICPMG 2026
11th International Conference on Physical Modelling in Geotechnics
8-12 June 2026, Zurich, Switzerland

Challenges in experimental modelling of pile-soil-tunnel interaction using a small diameter centrifuge

P. Yensri
School of Engineering, University of Birmingham, Birmingham, United Kingdom, pxy241@student.bham.ac.uk

A. Dobrisan
School of Engineering, University of Birmingham, Birmingham, United Kingdom
Schofield Centre, University of Cambridge, Cambridge, United Kingdom

A. Faramarzi, N. Metje, K. Hansard, C. Harbutt, E. Ashton
School of Engineering, University of Birmingham, Birmingham, United Kingdom

ABSTRACT: Protection of existing (buried) infrastructure is a key requirement when tunnelling in dense urban areas. Structures supported by pile foundations necessitate additional pile stability checks, as tunnelling in their proximity induces ground movements which can lead to increased axial forces, bending moments and displacements which may affect the integrity of the piles. Centrifuge modelling is a widely adopted technique for investigating the impact of tunnelling on adjacent piles. It offers several advantages, including the ability to accurately replicate the stress-strain behaviour of the prototype problem, whilst being cost effective and repeatable. However, careful consideration of test preparation techniques, scaling and instrument selection and accuracy is essential since errors are magnified due to the small values being measured. This paper discusses the challenges associated with using the small, 1.5 m diameter centrifuge in the National Buried Infrastructure Facility (NBIF) at the University of Birmingham to study pile-soil-tunnel interaction. Key hurdles identified and discussed in this study include: (a) inaccuracies introduced by the pluviation technique and assessing the relative density and, (b) the difficulty in controlling the tunnel volume losses of the small model and (c) selection of high precision instrumentation to obtain reliable data given the small package size. Careful pluviation using a movable support was adopted to achieve the relative density of 70%.

1 INTRODUCTION

Tunnelling in urban areas has increased rapidly to support expanding infrastructure needs in major cities, including transportation, water supply, drainage, and power distribution. This growing demand has resulted in tunnels being constructed in close proximity to existing piles supported structures, raising concerns regarding their structural integrity and serviceability due to tunnelling-induced ground movements, including pile displacement and induced forces (Basile, 2014).

Extensive research has been undertaken to better understand the complex pile–soil–tunnel interaction and mitigate associated risks, employing numerical, analytical, and physical modelling approaches. Among these, centrifuge modelling has become a widely adopted method for evaluating tunnelling effects on piled foundations. In recent years, small-radius centrifuges (with a beam radius of approximately 2 m) have become available at several research institutions, including the University of Nottingham, University of Sheffield, University of Dundee, City University of London, University of Western Australia and ETH Zurich. However, published centrifuge investigations of pile–tunnel interaction have predominantly been conducted using large-capacity centrifuge facilities (e.g. Jacobsz et al., 2004; Lee and Chiang, 2007; Marshall, 2009), which typically allow larger model dimensions and greater flexibility in instrumentation. To date, no published study has explicitly reported centrifuge modelling of pile–tunnel interaction using a relatively small-radius centrifuge (i.e. 0.75 m). The present study therefore contributes to the literature by demonstrating the feasibility and associated constraints of such an approach. Such a compact configuration introduces several additional challenges, including restricted working space for model construction, difficulties in achieving and verifying target relative densities, limitations in precise sand pluviation control, and the need to employ high-precision instrumentation.

This paper presents and discusses the challenges associated with conducting small-diameter centrifuge tests at the National Buried Infrastructure Facility (NBIF), University of Birmingham, to investigate tunnelling effects on existing piles. The study evaluates observed ground and pile settlements together with induced bending moments during swing-up and during included volume losses. The overall findings aim to assess the feasibility and research potential of small-diameter centrifuge modelling as a platform for advancing future investigations into soil–structure interaction, particularly in scenarios involving tunnels constructed in close proximity to pile foundations.

2 CENTRIFUGE MODELLING

In this study, centrifuge modelling was carried out using a 1.5 m-diameter beam-arm centrifuge (Broadbent GT6) located at the National Buried Infrastructure Facility (NBIF), University of Birmingham (Figure 1). The centrifuge is capable of accelerating models up to 300 g. The physical model was housed within a rigid aluminium strong-box cradle with internal dimensions of 300 mm length, 110 mm width, and 180 mm height. A transparent Perspex (PMMA) window was installed on one side of the cradle to facilitate direct observation of ground movements, while the opposite side accommodated the tunnelling system used to simulate excavation-induced volume loss. A counterbalanced cradle was mounted on the opposite end of the beam to minimise vibration during testing, ensuring the differential bending moment remained within the centrifuge's maximum allowable limit of 5 kgm.

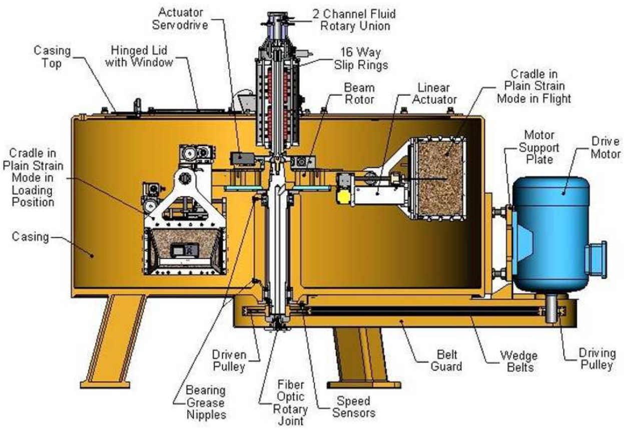

Figure 1. Centrifuge machine GT6 model

The data acquisition system comprised a Raspberry Pi 4 Model B computer integrated with an MCC128 DAQ HAT, providing eight available sensor channels. Custom Python scripts were developed to support the experiment, enabling (i) acquisition of signals from strain gauges, LVDTs, and pressure sensors, (ii) operation of a solenoid valve within the tunnelling system via a relay switch, and (iii) image capture using a Raspberry Pi camera positioned against the PMMA window to monitor soil conditions during pluviation and flight. The centrifuge test was operated at a target acceleration of 150 g, equivalent to approximately 450 rpm. This g-level was selected to represent prototype conditions corresponding to a 6.0 m tunnel diameter and a 1.2 m pile diameter.

2.1 Materials

2.1.1 Sand

In this study, fine sand was used to simulate the ground surrounding the pile. A particle size distribution (sieve analysis) was performed, indicating an average grain size (D_{50}) of 0.27 mm, as shown in Figure 2.

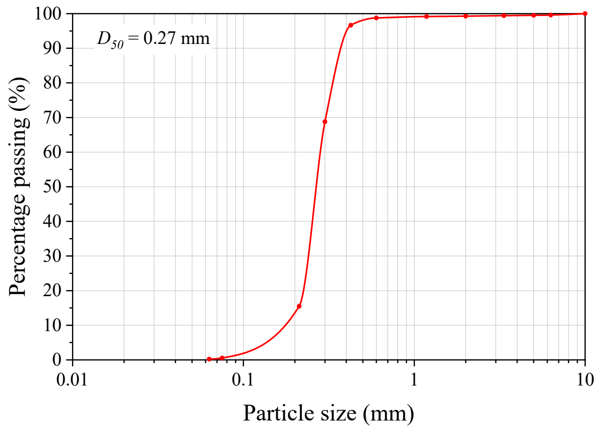

Figure 2. Grain-size distribution curve of the sand

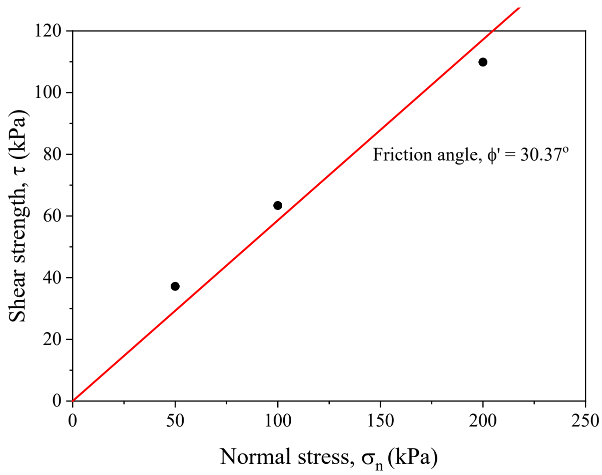

Figure 3. Shear test results of the sand

This sand was selected to satisfy the recommended criterion relating pile diameter (D_t) to D_{50}, as proposed by Madabhushi (2015), which suggests that D_t/D_{50} should exceed 10–15 to maintain continuity of the soil medium in small-scale soil–structure interaction tests (Clarkson et al., 2023). The current experimental configuration achieved a D_t/D_{50} ratio of 25.93, which lies comfortably within the recommended range. Shear tests were also carried out to obtain the shear strength parameters of the selected sand. Figure 3 illustrates the shear test results under normal stresses of 50, 100, and 200 kPa. From these tests, an effective friction angle (φ') of 30.4° was determined, together with negligible effective cohesion ($c' \approx 0$ kPa).

2.1.2 Modelled pile and tunnel.

For the modelled pile, the material selection was based on achieving an equivalent axial stiffness (EA) of 31,670 MN and bending stiffness (EI) of 2,850 MN·m² at prototype scale, corresponding to a 1.2 m diameter reinforced concrete pile. To replicate these properties, aluminium with an elastic modulus of 70 GPa and an outer and inner diameter of 7.0 mm and 5.0 mm, respectively, was selected. This choice also accommodated the physical constraints of the strong-box, ensuring sufficient clearance for installation while providing adequate surface area for mounting strain gauges. The model pile was fixed in position prior to sand placement using thin wires to maintain alignment. A spirit level was used to verify verticality and avoid unintended forces or displacements arising from pile inclination.

The mechanism of the model tunnel used in this study is based on those adopted by Jacobsz et al. (2004) and Divall (2013). The model tunnel comprised an aluminium core with a diameter of 34.0 mm, encased in a 1.0 mm thick rubber membrane, giving a final outer diameter of 40.0 mm when filled with water. Supporting wires were placed beneath the tunnel invert to prevent sagging due to water weight and to preserve the intended tunnel geometry. The tunnel was installed across the width of the strong-box and buried at a fixed depth of 135.0 mm, measured from the surface to the tunnel axis, corresponding to a 6.0 m tunnel diameter at a prototype depth of 20.25 m under 150 g scaling.

2.2 Pressurised tunnelling simulation

To maintain the tunnel geometry during the swing-up phase of centrifuge acceleration, a constant-head standpipe system was adopted. The water level within the standpipe was adjusted to equilibrate the in-situ overburden stress at the tunnel axis under centrifugal loading. Owing to the radial acceleration field in the centrifuge, the g-level varies along the vertical extent of the standpipe, resulting in a non-uniform stress distribution between its top and bottom elevations. Therefore, an equivalent g-level (N_{eq}) of 144g was determined to represent the average stress condition at the tunnel axis. The value of N_{eq} was calculated using equation 1:

$$N_{eq} = \frac{\omega^2}{Z_{model} g} \int_0^{Z_{model}} \left(Z_{top} + Z_{model}\right) dZ \quad (1)$$

Hence, the overburden pressure acting at the tunnel axis level can be estimated as follows:

$$N_{eq} \times \gamma_w \times H_s = N_{eq} \times \gamma'_{sand} \times Z = 314kPa \quad (2)$$

where N_{eq} is the equivalent g-level, ω (rpm) is the rotational speed, γ_w (kN/m^3) is the unit weight of water, H_s (m) is the height of water in the standpipe, γ'_{sand} (kN/m^3) is the unit weight of sand, Z_{top} (m) distance from centre of rotation to the ground surface level. and Z_{model} (m) is the depth of tunnel measuring from ground surface.

A solenoid valve was installed between the standpipe and the model tunnel to allow disconnection once the target g-level was reached. Subsequently, volume loss was simulated by extracting water from the tunnel through a small opening in the tunnel core, causing a reduction in tunnel diameter and inducing inward movement of the surrounding soil. Water removal was controlled by a volume-regulated chamber. Prior to swing-up, the piston within the chamber was positioned at the top, connected directly to the tunnel. Air pressure equivalent to the overburden pressure at the tunnel axis was applied to the underside of the piston to stabilise the tunnel, preventing premature deformation and avoiding water loss during swing-up. This pressure equilibrium was maintained throughout the spin-up to 150 g.

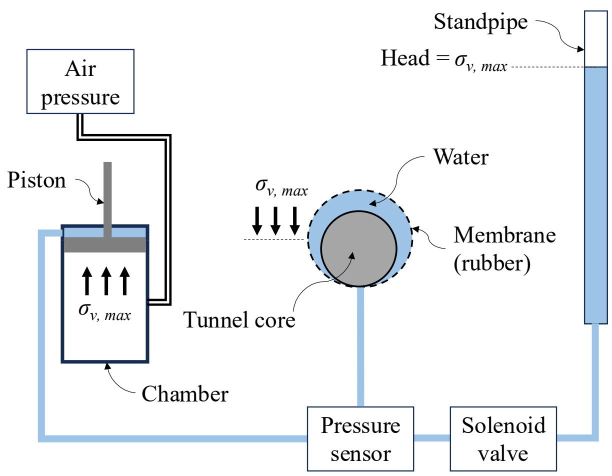

Figure 4. Pressurise tunnelling simulation system

Once the target g-level was achieved, the solenoid valve was closed, and the air pressure was gradually reduced, allowing the piston to descend and withdraw water from the tunnel, thereby simulating volume loss. A schematic of the tunnelling system used in this study is presented in Figure 4.

2.3 Preparation of the sand

Initially, the sand used in this test was mixed with dyed sand to provide visual texture for image analysis. The mixture comprised 15% black-dyed sand, coloured using food dye, blended with 75% untreated sand. Ground conditions were replicated using a pluviation (sand pouring) technique. The strong-box cradle was positioned on a trolley equipped with a height-adjustable lifting platform, enabling control of drop height to form uniform layers. Sand was poured from a horizontally moving nozzle, and four layers were deposited to maintain consistent drop height and achieve a uniform relative density throughout the depth. To ensure consistent relative density, each layer was weighed individually following deposition. The measured dry density was 16.17 kN/m³, corresponding to a relative density of 71.56%.

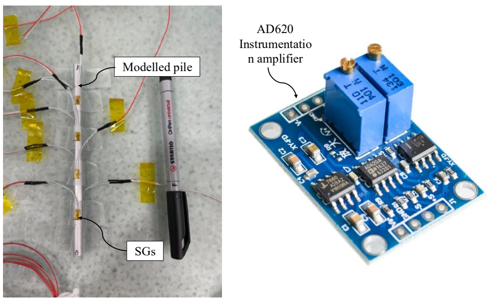

Figure 5. Mounted SGs on the pile and the AD620

2.4 Sensors

Four types of sensors were employed in the experiment to investigate the ground–structure response to bored tunnelling simulation: displacement transducers (LVDTs), strain gauges (SGs), and cameras.

2.4.1 Strain gauges

Four pairs of strain gauges were mounted on the surface of the model pile in a half-bridge configuration, enabling measurement of induced bending moments while eliminating the influence of axial strain. The strain gauge pairs were positioned at four prototype depths: 4.5 m, 9.0 m, 13.5 m, and 18.0 m. Additionally, an AD620 instrumentation amplifier was employed to amplify the voltage output from the gauges. Figure 5 shows the strain gauge installation on the model pile and the corresponding AD620 amplifier module used in this study.

2.4.2 Displacement transducer

For this experimental programme, three LVDTs were installed. The first (LVDT1) was positioned at the ground surface above the tunnel axis to measure maximum surface settlement induced by tunnelling. The second (LVDT2) was mounted at the pile head to record pile settlement. The third (LVDT3) was attached to the piston chamber to monitor piston movement during the simulated volume-loss process (see Figure 6a).

2.4.3 Cameras

The Raspberry Pi Camera Module 2 was used to capture images during flight. The camera was mounted on a support in front of the PMMA window, positioned approximately 20 cm away, enabling it to record the zone of influence expected to be affected by tunnelling.

2.5 Model preparation

A schematic of the model preparation and testing sequence is presented in Figure 7. The set-up commenced by weighing the empty strong-box cradle, containing the model pile in its final position but without sand, to establish the initial reference mass. Sand was then pluviated in layers to progressively construct the soil profile. After the second layer was placed, the supporting wires beneath the tunnel were carefully removed, as the surrounding sand provided sufficient lateral confinement to maintain tunnel geometry and prevent distortion of the water-filled membrane. Pluviation continued in a controlled manner until the final layer was deposited. The wire suspending the pile was removed immediately after the final pour, ensuring vertical alignment and avoiding bending or rotation during deposition. Following sand placement, the cradle was reweighed to determine the mass of sand and calculate the final dry density, confirming that the target relative density had been achieved. The LVDTs were then installed at their designated positions using custom 3D-printed sockets to ensure stable positioning and accurate measurement alignment. A full working load was not applied due to space constraints. However, Lee and Chiang (2007) demonstrated that, in the absence of an applied working load, the maximum bending moment induced by tunnelling does not differ significantly from that observed in a loaded pile, when considering a similar relative pile–tunnel depth.

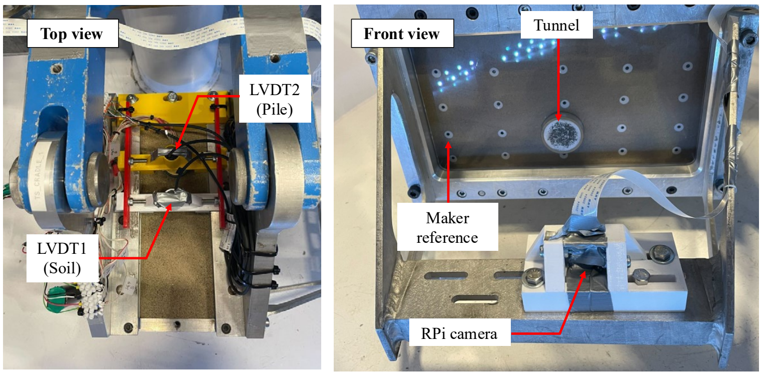

(a)

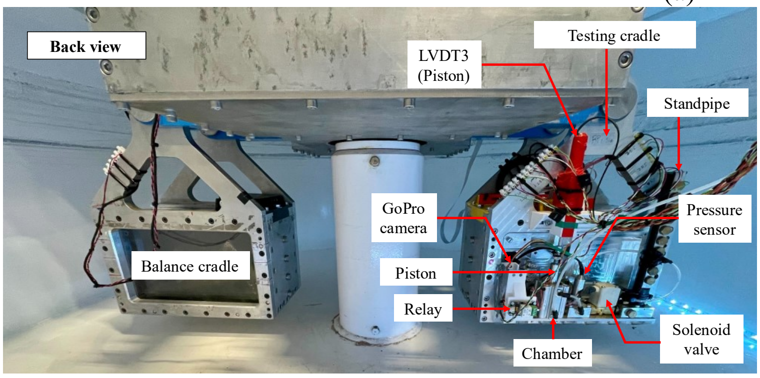

(b)

Figure 6. Test setup and instrumentation

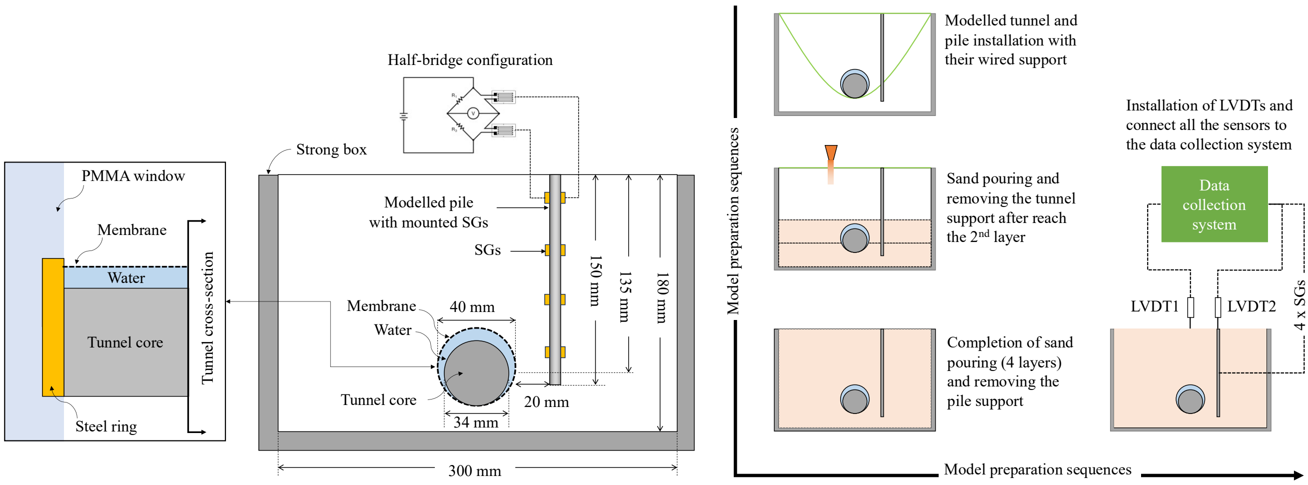

Figure 7. Test preparation schematic diagram

3 TEST PROCEDURE

After completion of the model preparation, the test commenced by applying an air pressure of 350 kPa to the underside of the chamber piston (see Figure 4) to counteract the pressure exerted from the tunnel and chamber components at g, and prevent premature volume loss. The swing-up phase was then carried out to reach the target acceleration of 150 g. During this period, the solenoid valve remained open to maintain internal tunnel pressure, and all sensors were activated to capture pile–soil response throughout swing-up.

Upon reaching 150 g, the solenoid valve was closed, and air pressure was gradually reduced to initiate tunnel deformation. The pressure was first lowered to 250 kPa, producing an initial stage of volume loss. A further reduction to 200 kPa generated a second volume-loss increment. At this point, a pronounced piston movement occurred, bringing the piston reach to the chamber base and preventing further controlled extraction, leading to termination of the test and initiation of the swing-down phase.

Data acquisition was carried out separately for each stage of the experiment: swing-up, volume-loss generation, and swing-down, while also being recorded in a continuous global file. This dual-recording approach facilitated clearer data interpretation and minimised synchronisation ambiguity between test phases.

4 SOIL AND PILE RESPONSE TO GROUND MOVEMENTS DURING SWING-UP PHASE

This section reports and discusses the soil and pile responses to ground movements generated during the swing-up phase. Figure 8 shows the measured soil displacement above the tunnel axis and the corresponding pile movement, recorded by LVDT1 and LVDT2, respectively. At 150 g, a maximum soil surface settlement of approximately 0.60 mm was observed, whereas the pile experienced a slightly larger settlement of about 0.80 mm. The differential response is mainly attributed to the additional load of 100 g applied at the pile head, which induced extra downward displacement, while the soil settlement captured by LVDT1 reflects only the increase in vertical stress during spin-up. Other compounding factors, such as the shadow effect of the pluviation phase around the pile, might have contributed to the observed difference in settlement between pile and free field, but cannot be quantified with the available instrumentation.

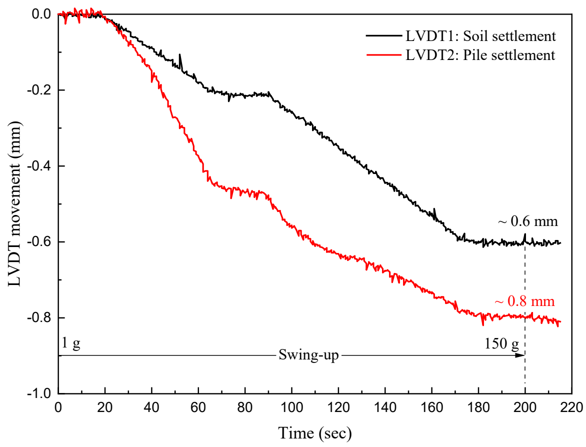

Figure 8. Soil and pile settlement during the swing-up phase

Figure 9 presents the bending moment profiles along the pile depth at the end of the swing-up phase. Negative bending moments were recorded at the top three strain gauge levels (SG1–SG3), while a positive moment was detected at SG4. Substantial uncertainties were noted, with estimated error ranges of ±107.71 kNm, ±101.32 kNm, ±67.05 kNm, and ±115.49 kNm for SG1, SG2, SG3, and SG4, respectively, corresponding to errors of approximately 25–50%. These results indicate that strain-gauge measurements under dynamic spin-up conditions may introduce significant error, highlighting the limitations of using SGs to capture bending response reliably during this stage of centrifuge testing.

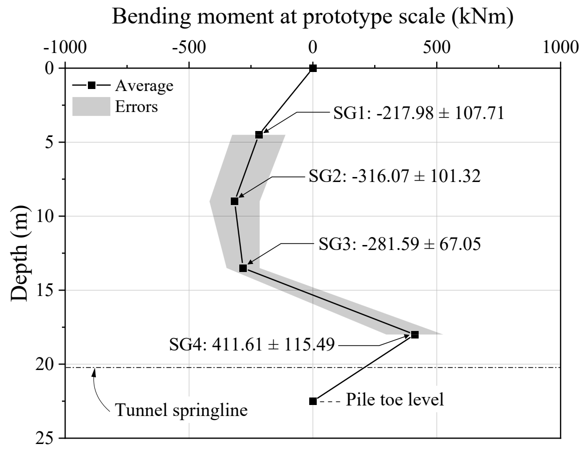

Figure 9. Induced bending moment and errors in measurement in the pile during the swing-up phase

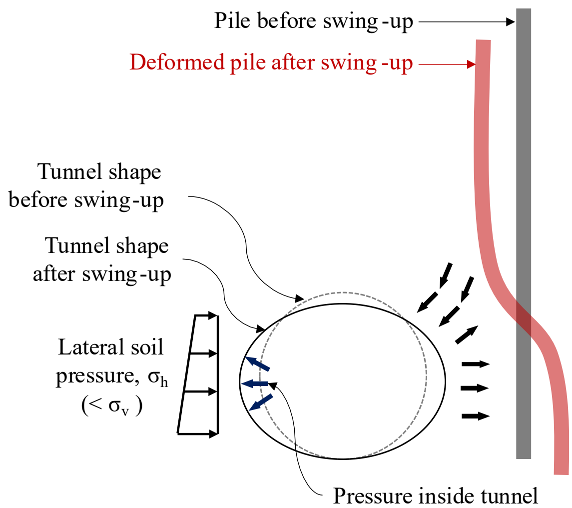

Figure 10. Tunnel deform shape during the swing-up phase

Additionally, the shape of the bending moment profile observed immediately after the swing-up process can be attributed to the interaction between the internal and external pressures acting on the tunnel. At the start of the test, the applied internal pressure of 350 kPa exceeded the lateral earth pressure exerted on the tunnel lining, as estimated using the coefficient of earth pressure at rest (K_0). This imbalance caused the tunnel to deform into a lateral oval shape (see Figure 10). The resulting distortion displaced the surrounding soil, pushing the pile laterally away from the tunnel between the tunnel crown and pile toe. In contrast, the upper part of the pile (from the head to approximately tunnel crown level) was drawn slightly toward the tunnel. The combined response can explain the bending moment distribution presented in Figure 9.

This observation confirms that applying pressure-controlled support to the tunnel in small-scale centrifuge modelling can induce an initial bending response in adjacent piles during spin-up. The behaviour reflects ground compression and dilation associated with tunnel deformation, demonstrating that measurable pile–soil–tunnel interaction occurs even prior to simulated volume loss.

5 SOIL AND PILE RESPONSE TO TUNNEL VOLUME LOSSES

This section reports and discusses the soil and pile responses to the simulated tunnelling-induced volume loss, including ground and pile settlement and the corresponding induced bending moment. Figure 11 compares the measured ground settlement trough with the empirical prediction, which can be calculated using the following equations proposed by Peck (1969):

$$S = S_{max} exp\left(-\frac{x^2}{2i^2}\right) \tag{3}$$

$$S_{max} = \frac{0.313 V_L D^2}{i} \tag{4}$$

$$i = K \times Z_{tunnel} \tag{5}$$

where S_{max} is maximum settlement, S is surface settlement at a transverse distance x from the tunnel centre line, i is point of inflexion, x is the distance from tunnel centre line, V_L is volume loss, D is tunnel diameter, K is trough width parameter and Z_{tunnel} is tunnel depth.

The settlement trough derived from the empirical equation is controlled by the point of inflexion, governed by the dimensionless trough width parameter, *K*. Since only one LVDT measurement is available, *K* is inferred based on the work of Mair and Taylor (1997) who reported that *K* for granular materials typically ranges between 0.25 and 0.45. Using these K bounds we can compute the likely range for the free field settlement and compare with the measured pile settlement. The lower bound *K* = 0.25 yields pile displacements approximately equal to surface settlements for both first and second stages. Upper bound *K* = 0.45 provides the expected interpretation of the soil–pile response, aligning with the "zone of influence" concept (Kaalberg et al., 2005; Selemetas, 2005), whereby piles extending below the tunnel axis undergo reduced settlement relative to the ground surface. Overall, a *K* within the probable bound of 0.25 to 0.45 implies a soil settlement in excess of the pile movement, in agreement with expected behaviour (see Figure 11).

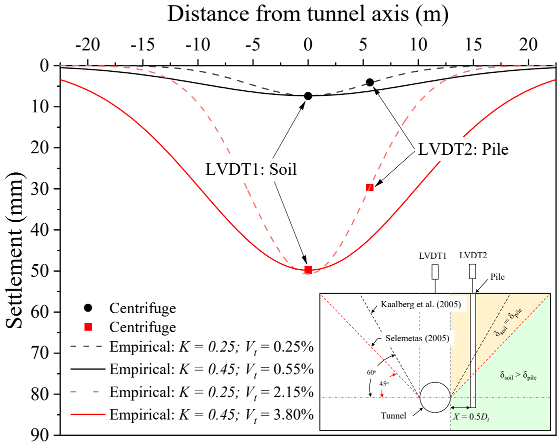

Figure 11. Ground surface and pile settlement caused by tunnelling simulation

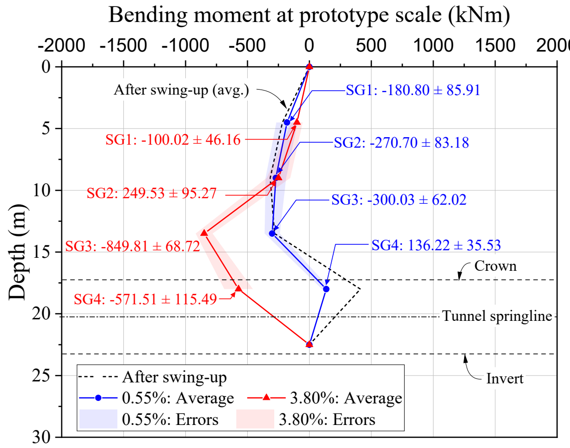

Figure 12. Induced bending moment and errors in measurement in the pile caused by tunnelling.

Figure 12 presents the bending moment profiles in the pile for different levels of volume loss during tunnelling simulation. After the first stage (0.55%), the profile indicates a clear shift, showing that the pile moved predominantly towards the tunnel. This resulted in a reduction in bending moment, particularly at SG4, located closest to the tunnel axis and therefore most strongly affected. A similar trend is observed at 3.80% volume loss, where the bending moment change becomes more pronounced, especially at SG3 and SG4 near the tunnel crown and axis, respectively. These positions experienced the greatest influence from tunnelling-induced ground deformation.

With respect to relative error, a clear trend was observed. The bending moment errors recorded from the strain gauges decreased noticeably after the swing-up phase, particularly for gauges subjected to significant bending due to tunnelling (SG2, SG3, and

SG4). Figure 13 plots the percentage error against the average bending moment for each gauge. During swing-up, errors ranged from approximately 25–50%. After the 0.55% volume loss, the errors across all the SGs slightly reduce from the swing-up phase approximately 1–3%. However, once the relatively large volume loss of 3.8% was generated, the gauge SG3 and SG4 exhibited a dramatic reduction to approximately 8% and 17%, respectively. This behaviour reflects the nature of relative error: as bending moment increases, the measurement grows faster than the associated uncertainty, reducing the error proportion. As a result, strain gauges provide more reliable data at higher deformation, while greater relative error occurs during low-strain stages such as swing-up.

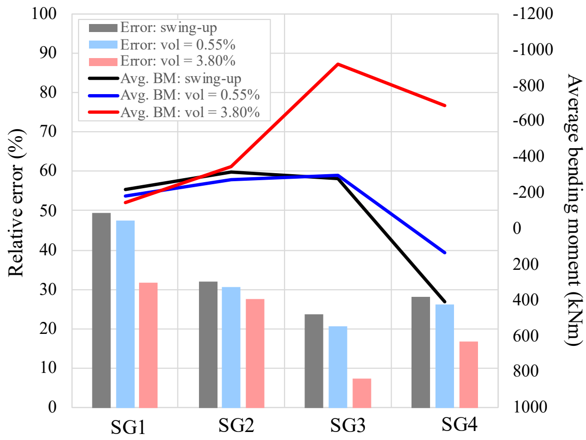

Figure 13. Percent errors of strain measurements

6 CONCLUSIONS

Based on the successful small-diameter centrifuge modelling, to investigate tunnelling effects on existing piles, the following conclusions can be drawn:

- Layered sand placement achieved relative densities >70%, resulting in minimal swing-up ground movement and no significant change in density under high g-level.
- Detectable pile bending developed during swing-up due to pressure imbalance between the interior tunnel support pressure and external earth pressure, demonstrating that soil–pile interaction is initiated prior to any volume loss.
- Measurement errors in strain gauges were highest during low-strain swing-up conditions but decreased substantially once volume loss induced significant pile deformation, indicating improved reliability under higher bending demand.
- All sensors and the microcontroller system (Raspberry Pi) operated reliably and produced coherent measurements under high g-levels.
- Centrifuge results matched empirical, expected settlements providing the viability and accuracy of centrifuge tests even on small diameter devices.

ACKNOWLEDGEMENTS

The authors are grateful for the support and funding provided by the National Buried Infrastructure Facility, School of Engineering, The University of Birmingham (grant reference number: EP/P013635/1).

REFERENCES

Basile, F. (2014). Effects of Tunnelling on Pile Foundations. *Soils and Foundations*, 54(3), pp. 280-295. https://doi.org/10.1016/j.sandf.2014.04.004

Clarkson, C., Eichhorn, G. and Siemens, G. (2023) Centrifuge modellinf of axially loaded steel piles in cold and thawing frozen sand. *Internatipnal Journal of Physical Modelling in Geotechnics*. https://doi.org/10.1680/jphmg.22.00062

Divall, S. (2013). *Ground movements associated with twin-tunnel construction in clay*, PhD thesis, City University London, London, UK.

Jacobsz, S.W., Standing, J.R., Mair, R.J., Hahiwara, T. and Suiyama, T. (2004). Centrifuge modeling of tunnelling near driven piles. *Soils and Foundations*, 44(1), pp. 49-56. https://doi.org/10.3208/sandf.44.49

Kaalberg, F. J., Teunissen, E. A. H., van Tol, A. F. and Bosch, J. W. (2005). Dutch research on the impact of shield tunnelling on pile foundations. *Proceedings of the 5th International Symposium on Geotechnical Aspects of Underground Construction in Soft Ground*, pp. 123-131. https://doi.org/10.3208/sandf.44.49

Lee, C.J. and Chiang, K.H. (2007). Responses of single piles to tunnelling-induced soil movements in sandy ground. *Canadian Geotechnical Journal*. 44, pp. 1224-1241. https://doi.org/10.1139/T07-050

Madabhushi, S. P. G. (2015). Centrifuge Modelling for Civil Engineers. *CRC Press/Balkema*, Leiden, the Netherlands.

Mair, R.J. and Taylor, R.N. (1997). Bored tunnelling in the urban environment, *Proceedings of the Fourteenth International Conference on Soil Mechanics and Foundation Engineering*, Vol.4, pp. 2353- 2385.

Marshall, A.M., (2009). *Tunnelling in sand in its effects on pipelines and piles*. PhD thesis, University of Cambridge, Cambridge, UK.

Peck, R. B. (1969). Deep excavations and tunnelling in soft ground. *7th International Conference on Soil Mechanics and Foundation Engineering*, 225-290. Mexico City.

Selemetas, D. (2005). *The response of full-scale piles and piled structures to tunnelling*. PhD thesis, University of Cambridge, Cambridge, UK.